Proton Induced Reactions of Thorium—Fission Yield Curves*

HOWARD A. TEWES† AND RALPH A. JAMES
Department of Chemistry, University of California, Los Angeles, California
(Received June 30, 1952)

The fission yields of a number of nuclides produced in proton-induced fission of Th^{232} were determined at several proton energies in the range of 6.7 Mev to 21.1 Mev. At the same time, the relative cross sections of the (p,n) and $(p,3n)$ reactions on Th^{232} were also determined. It was found that, although the fission reaction was predominant at proton energies greater than 8 Mev, competition from the (p,xn) type of reaction was considerable over all energies investigated.

The trough in the fission yield curve becomes shallower with increasing proton energy and this change was quantitatively determined over the energy range investigated. A model is proposed to explain the change in shape of the fission yield curves.

An approximate determination of the excitation function for the (p,f) reaction was made; the shape of the resulting curve was at least qualitatively in agreement with the excitation function predicted from existing theory.

INTRODUCTION

DURING the past few years all of the work which has been done on the distribution of fission products originating in fission induced with high energy particles has indicated that the probability of symmetrical fission becomes greater at high energies.[1–4] However, none of this work has given fission yield curves of sufficient precision at various energies to give more than qualitative information about this trend toward greater symmetry in the fission process as the excitation energy is increased.

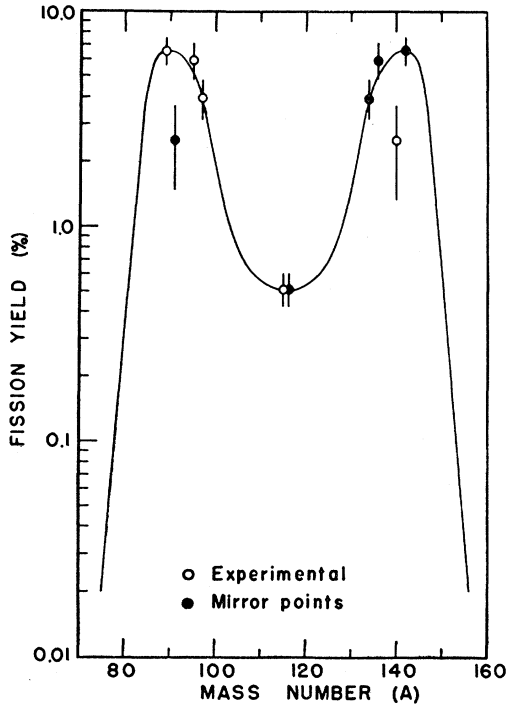

FIG. 1. Fission yield curve. Proton energy, 6.7 Mev.

Considerable work has also been done at very high particle energies which has indicated that the $(d,xnyp)$ and $(\alpha,xnyp)$, i.e., "spallation," reactions may compete favorably with fission,[2,4] but nothing has been published on the relative cross sections of this type of reaction with protons nor on the deuteron and helium ion induced reactions in the energy region just above the threshold for fission where the results would be expected to be more easily interpreted.

The work reported here was undertaken for the following purposes: (1) to ascertain the change in shape of the fission yield curve with increasing proton energies; (2) to determine the variation in the ratio of (p,f) to (p,n) and $(p,3n)$ reactions with increasing proton energies; and (3) to obtain the excitation functions for fission, the (p,n) and $(p,3n)$ reactions of thorium for proton energies below 21 Mev.

PROCEDURE

All bombardments were made on 0.001-in. or 0.002-in. thorium metal foil. As there was little possibility that any impurities could introduce errors in the determination of the expected bombardment products, no effort was made to analyze or purify the thorium. The targets were mounted on the unshielded probe of the UCLA frequency-modulated cyclotron; individual bombardments were obtained at selected proton energies by adjusting the position at which the target intercepted the beam. The irradiations varied from one to five hours in length with proton currents of approximately 0.1 microampere. In general, a 10- or 20-mg portion of carrier of the element being investigated was added to an aliquot of the hydrochloric acid solution of the target, the element was separated and purified from all others, and the chemical yield was determined by weighing a compound of the recovered carrier. The chemistry used

* This work was supported in part by the joint program of the ONR and AEC.

† Present address—California Research and Development Company, University of California Radiation Laboratory, Berkeley 4, California.

[1] A. S. Newton, Phys. Rev. **75**, 209 (1949).
[2] P. R. O'Connor and G. J. Seaborg, Phys. Rev. **74**, 1189 (1948).
[3] A. Turkevich and J. B. Niday, Phys. Rev. **84**, 52 (1951).
[4] R. H. Goeckermann and I. Perlman, Phys. Rev. **76**, 628 (1949).

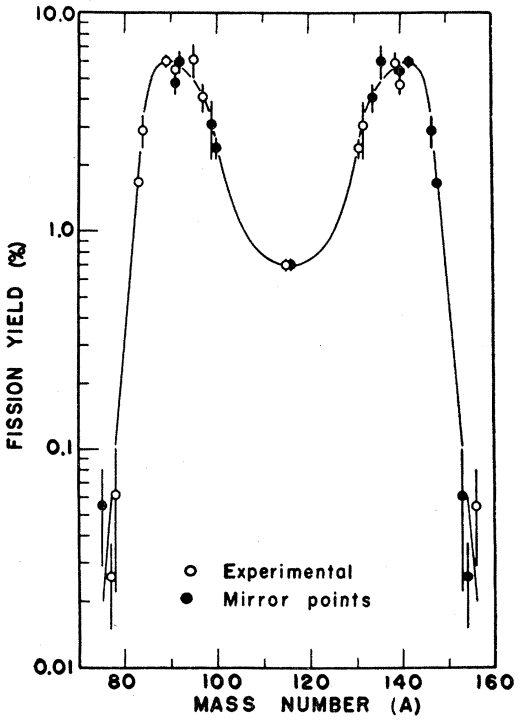

FIG. 2. Fission yield curve. Proton energy, 8.0 Mev.

has been discussed in detail by Meinke[5] and has also been described by other investigators.[1,3,4] An outline of these chemical procedures and a discussion of the nuclides identified are included in the appendix.

The final precipitates were transferred to $\sim$3 cm^2 area filter papers, which were subsequently mounted on chipboard sample cards and covered with 2.7-mg/cm^2 cellophane. Radiation measurements were made with a single lead-shielded Geiger-Müller tube with a 2.3-mg/cm^2 mica (end) window. The background radiation level was subtracted from all measurements; also coincidence corrections were made where high activities were encountered. Partial absorption curves were determined for all isotopes studied this work in order that counting rates could be corrected to zero absorber thickness.

RESULTS

Fission Yield Curves

The fission yield curves for protons ranging in energy from 6.7 to 21.1 Mev are given in Figs. 1 to 7, and Table I gives the data from which these curves were constructed. Figure 8 reproduces the fission yield curves obtained by Turkevich and Niday[3] with 2.6-Mev neutrons and by Newton[1] with 37.5-Mev helium ions, along with two of the curves obtained in this work so that a direct comparison can be made. In all of these curves open circles represent the experimental data, and solid circles represent mirror points.[6] The mass numbers of the mirror points (A') were obtained by assuming that two neutrons were given off in the fission process; consequently, $A'=231-A$. The number of neutrons assumed to be given off was arbitrarily chosen to give the smoothest curve in the regions where the fission yields were relatively high, and consequently, fairly reliable. The assumption that the average number of neutrons emitted is independent of the degree of symmetry of that particular fission is open to question. It may be noted that the fission yield curves obtained with proton energies of 18 Mev or less show appreciable scatter of points at the extreme ends of the curves. If, however, the expression used in calculating the mirror points is changed to $A'=233-A$, this scatter at the ends of the curves would be eliminated but would, naturally, introduce more scatter near the maxima. The scatter is completely eliminated if it is assumed that less neutrons are emitted in the very asymmetric fission (and possibly in symmetrical fission) than are emitted when the fission products are those of maximum yield.

Excitation Functions

Although it was not possible by the methods used here to determine accurately the absolute values of the cross sections for the reactions studied, the ratios of these cross sections at each energy were determined with fair precision as indicated by the data of Table I.

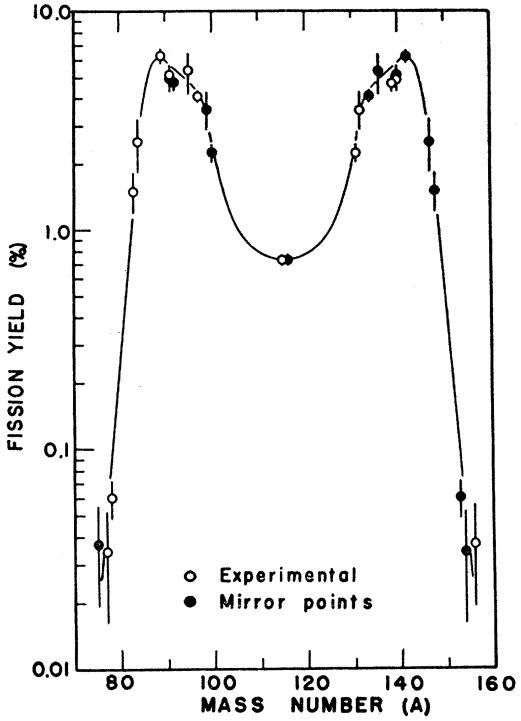

FIG. 3. Fission yield curve. Proton energy, 9.3 Mev.

[5] W. W. Meinke, AEC Reports AECD-2738 (UCRL-432) and AECD-2750 (unpublished).

[6] The use of both experimental and mirror points in the drawing of a fission yield curve is not uncommon; e.g., Turkevich and Niday (reference 3) constructed their fission yield curve in this way.

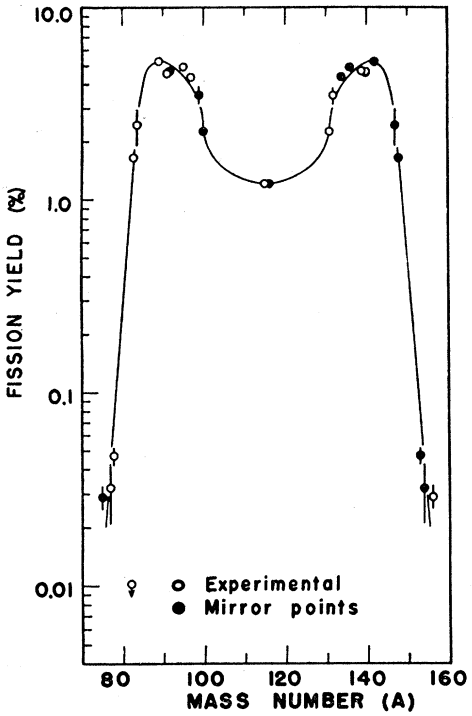

FIG. 4. Fission yield curve. Proton energy, 13.3 Mev.

In order to have some scale on which to present these ratios, the statistical treatment of Weisskopf[7,8] has been used to calculate the total cross section for proton induced reactions of thorium. In Fig. 9 the points were plotted by using the observed ratios and the total calculated cross section at each energy. The cross section of the $(p,2n)$ reaction was not determined but was arbitrarily assumed to have the form indicated. It is unlikely that other reactions such as (p,p); (p,pn); (p,α), etc. have cross sections large enough at the energies involved here to have any appreciable effect on these curves. The cross sections were also calculated in the usual manner from the yield and the (very inaccurately) measured beam striking the unshielded probe in the cyclotron tank. In most cases the results are of the same order of magnitude as those shown in Fig. 9, but large discrepancies were present in certain instances

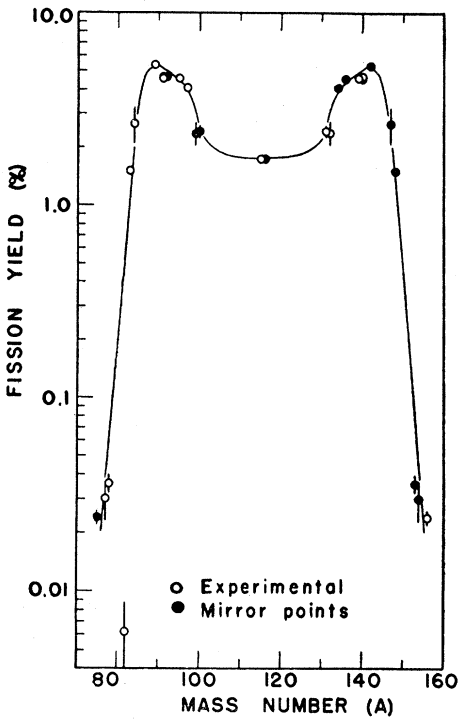

FIG. 5. Fission yield curve. Proton energy, 17.8 Mev.

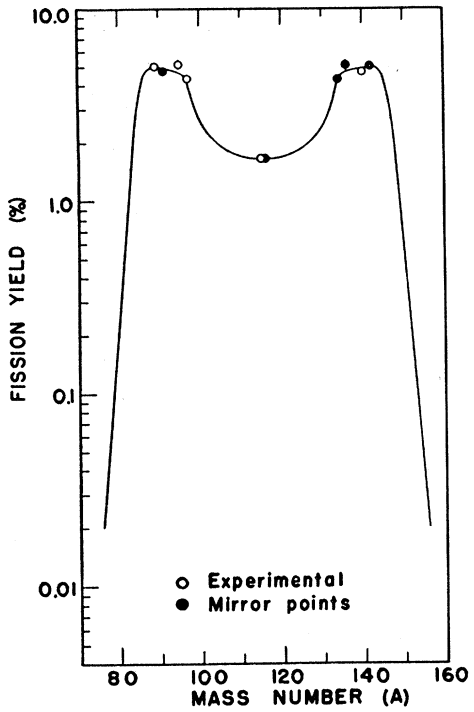

FIG. 6. Fission yield curve. Proton energy, 19.5 Mev.

which are best explained by the large error in proton beam measurement.

It should be noted that, although the (p,f) reaction is predominant at higher particle energies, the (p,xn) reactions account for much of the total proton cross section at all energies. It is highly probable that this is the case for the interaction of any charged particle with heavy nuclei; consequently, the abnormally low fission cross sections which have been observed by Jungerman for helium ions on thorium[9] can reasonably be attributed to the competition of (α,xn) reactions.

A picture which is consistent with the above results on the excitation functions as well as the trend in

[7] V. F. Weisskopf and D. H. Ewing, Phys. Rev. **57**, 472 (1939).
[8] V. F. Weisskopf, unpublished lecture series on nuclear physics (Los Alamos Report No. 24), p. 207.
[9] J. Jungerman, Phys. Rev. **79**, 632 (1950).

degree of symmetry of fission is presented in the discussion of these results.

Miscellaneous Results

It was found that the ratio of the yields of the two Cd^{115} isomers remained approximately constant over the range of energies at which this quantity could be measured. The average value of the ratio (2.19 day/43 day) in eight bombardments in the energy range 13.3–21.1 Mev was 16.7, the extreme values being 15.1 and 17.4 with no observable trend with increasing energy. It seems probable that all of both of these isomers are formed from a primary fission product of lower Z and that this ratio represents the natural ratio arising from decay of Ag^{115}. It is doubtful that the value 16.7 obtained in this work represents a significant departure from the value 14 quoted in the slow neutron fission of uranium,[10] particularly since the half-life of 2.19 days used here differs from that used in calculating the ratio in slow neutron fission.

The fraction of the As^{77} which was formed by the decay of the 59-second Ge^{77} was calculated for those bombardments where sufficient arsenic activity was present to make the computations meaningful. These values were constant within experimental error, the mean value for the ratio (59-sec Ge^{77})/(12−hr Ge^{77}) being 1.1 ± 0.2 Here again it is probable that this is the ratio of Ge^{77} isomers resulting from the decay of Ga^{77}.

DISCUSSION OF RESULTS

With regard to the series of fission yield curves resulting from the present investigation, several points are of interest. First, the depth of the trough decreases markedly and in a regular fashion with increasing energy of the incident protons. This trend is clearly shown in Table II and also in Fig. 10 where the ratio of the fission yield of Cd^{115} (the sum of the two isomers) to the yield of Sr^{89} is plotted against the proton energy.

Newton's results[1] are somewhat inconclusive with respect to the depth of the trough; however, the reported ratio of Cd^{115}/Sr^{89} is of the order of 0.5, which is not inconsistent with the value which might have been predicted for 37.5-Mev particles on the basis of this curve. It may be noted that if the Cd^{115}/Sr^{89} yield ratio determined by Turkevich and Niday[3] for the fission of thorium with pile neutrons is plotted in Fig. 10, it lies on the extrapolated curve within experimental error. Consequently, it may be concluded that the nature of the particle which induces fission as well as the nucleus which is considered to be the compound nucleus are not as critical in determining the mode of fission as is the energy imparted to the compound nucleus by the particle.

If one assumes that a compound nucleus is formed with excitation energy determined by the energy of the incident particle and that this compound nucleus may lose its excess energy by the numerous possible modes of fission or by the emission of one or more neutrons, the fraction decomposing by any particular mechanism would then be proportional to the relative rate of that

[10] The Plutonium Project, J. Am. Chem. Soc. 68, 2411 (1948).

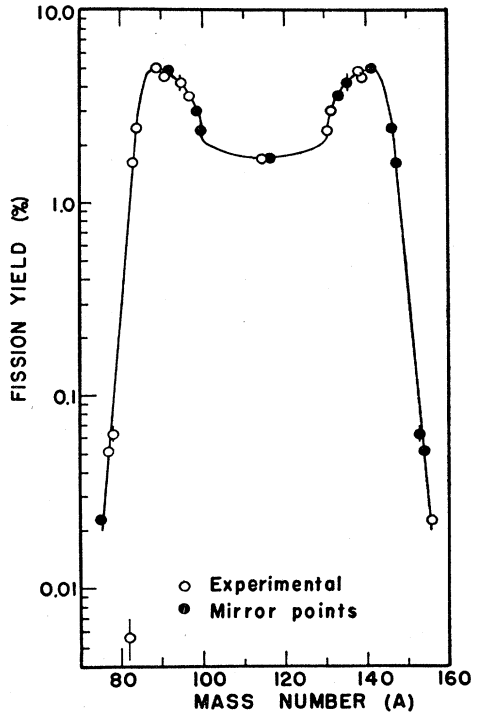

FIG. 7. Fission yield curve. Proton energy, 21.1 Mev.

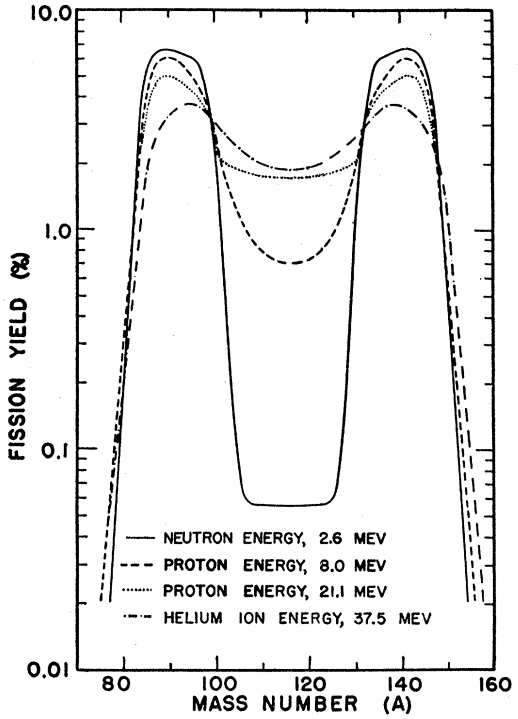

FIG. 8. Fission yield curves for Th^{232}.

TABLE I. Nuclide yields, percent (total atoms fissioned = 100 percent).

Mass No.	Proton energy (Mev) 6.7	8.0	9.3	13.3	17.8[a]	19.5[a]	21.1
77		0.026±0.011	0.034±0.018	0.032±0.011	0.030 ±0.007		0.052 ±0.006
78		0.061±0.039	0.060±0.012	0.047±0.005	0.036 ±0.004		0.064 ±0.006
82				0.010_3 (Max)	0.0062±0.0025		0.0057±0.0014
83		1.67 ±0.07	1.51 ±0.32	1.65 ±0.08	1.51 ±0.07		1.64 ±0.07
84		2.90 ±0.50	2.53 ±0.69	2.44 ±0.53	2.66 ±0.56		2.49 ±0.50
89	6.55±0.96	6.00 ±0.37	6.24 ±0.49	5.25 ±0.18	5.31 ±0.12	5.01±0.14	5.07 ±0.14
91		5.48 ±0.53	5.15 ±0.52	4.58 ±0.21	4.57 ±0.28		4.61 ±0.14
95	5.93±1.14	6.05 ±1.05	5.29 ±1.10	4.93 ±0.18	4.57 ±0.22	5.14±0.32	4.27 ±0.38
97	3.97±0.84	4.08 ±0.61	4.07 ±0.24	4.36 ±0.11	4.08 ±0.15	4.32±0.20	3.63 ±0.09
115	0.51±0.09	0.69 ±0.03	0.73 ±0.04	1.22 ±0.04	1.75 ±0.11	1.66±0.10	1.74 ±0.07
131		2.40 ±0.24	2.24 ±0.22	2.27 ±0.07	2.45 ±0.18		2.38 ±0.05
132		3.03 ±0.90	3.56 ±0.72	3.48 ±0.35	2.38 ±0.34		3.02 ±0.24
139		5.95 ±0.68	4.75 ±0.41	4.72 ±0.18	4.63 ±0.22		4.96 ±0.29
140	2.49±1.16	4.74 ±0.53	4.90 ±0.61	4.61 ±0.11	4.67 ±0.23	4.71±0.22	4.51 ±0.07
156		0.055±0.026	0.037±0.018	0.029±0.004	0.024 ±0.002		0.023 ±0.001
Pa^{233}					1.31 (Max)	38.8 ±1.8	31.1 ±1.7
Pa^{232}	147 ±4	116 ±17	34.3 ±5.3	5.08 ±0.75	2.64 ±0.40	0.88±0.14	0.81 ±0.12

[a] Fission yields quoted are averages of three separate bombardments at this energy.

reaction. These rates may in turn be considered to be determined by the height of a potential "barrier" characteristic of that particular reaction. The rate and therefore the cross section for each reaction would then be given by the expression $\sigma_i = ce^{-E_i/E}$, where σ_i is the cross section for a particular reaction (as for example fission into two nuclei of masses 115 and 116); c is a constant which depends on the target nucleus, the bombarding particle, and the energy of the incident particles; E_i is the height of the barrier for reaction i and E is the excitation energy. If we now take the ratio of cross sections for two particular reactions at a given energy, we get the expression $\ln(\sigma_1/\sigma_2) = (E_2 - E_1)/E$. Figure 11 shows a plot of $\log(\sigma_1/\sigma_2)$ *vs* $1/E$, where σ_1 is the cross section for production of Cd^{115} and σ_2 is the cross section for production of Sr^{89}, with E equal to the proton energy in the range of 6.7 to 21.1 Mev. It will be observed that the points fall on a straight line. The slope of this line gives for $E_2 - E_1$, i.e., the difference in height of the "barrier" for these two reactions, a value of 15 Mev. The plot becomes very insensitive to changes in energy on the high energy region, so it may or may not be significant that the value 0.5 for the ratio of these cross sections found by Newton[1] with 37.5-Mev helium ions also falls on the straight line within experimental error. The point obtained by Turkevich and Niday[3] for pile neutrons would appear to be rather far from the line if we use the value of 2.6 Mev for the effective neutron energy. However, a change to only 3.4 Mev for this effective energy brings this point to the line, and this value does not seem to be unreasonable since the authors estimated that half of the fissions were caused by neutrons of energy greater than 2.7 Mev. The compound nucleus is also different, of course, when helium ions or neutrons are the incident particles, so exact agreement could not be expected.

A second point of interest regarding the fission yield curves is the apparent presence of a secondary maximum in the yield curves at $A = 95$ and $A = 136$. This secondary maximum effect has been previously noted in the thermal neutron fission of U^{235}. Glendenin *et al.*[11] have conclusively shown by means of a mass spectrometric study that maxima exist at $A = 98$–100 and $A = 133$–136 in the fission yield curve. The maximum in the heavy fragment region was attributed by these workers to the stable 82-neutron configuration; the other maximum necessarily resulted from the nature of the fission process. Since the stabilizing effect of closed shells on fission yields would be expected to become of less importance as the excitation energy of the fissioning nucleus was increased, it is not surprising to note that the secondary maximum becomes less pronounced as as proton energies are increased.

The apparent flatness of the fission yield curves in the region of nearly symmetric fission is especially evident in those cases where high energy protons were used. It is probable, however, that this flatness would also be exhibited in the fission yield curves obtained with low energy particles, but the effect cannot be conclusively demonstrated since only one point was taken in the minimum yield region at each proton energy. The curve obtained by Turkevich and Niday[3] also shows this flat minimum. The effect has also been demonstrated with fast (pile) neutrons on U^{238}.[12] Apparently, only with slow neutron induced fission is there a sharp fission yield rise about a minimum symmetric point. These results are in agreement with the hypothesis that the energy barrier for symmetric or near symmetric fission is somewhat higher than that for asymmetric fission. This barrier is apparently quite uniform in height in the region where the fission

[11] Glendenin, Steinberg, Inghram, and Hess, Phys. Rev. 84, 860 (1951).

[12] Engelkemeir, Seiler, Steinberg, and Winsberg, *Radiochemical Studies: The Fission Products* (McGraw-Hill Book Company, Inc., New York, 1951), Paper No. 218, National Nuclear Energy Series, Plutonium Project Record, Vol. 9, Div. IV.

fragments produced have mass numbers ranging from about 103 to 128. For the fission processes in which fragments with masses 85–95 and 136–146 are produced, the barrier height is lower (probably of the order of 7 Mev), and for those fissions producing fragments at the extreme ends of the fission yield curve the barrier height approaches infinity. It should be noted that these barrier heights do not include the Coulombic repulsion of the nucleus for the bombarding particle but are concerned only with the possible modes of decomposition of the compound nucleus.

We are grateful to Professor J. R. Richardson for his interest and cooperation and to Mr. S. Plunkett and the cyclotron operating staff for the numerous bombardments.

APPENDIX

The chemical separation method and isotope identification for each element investigated are given briefly. In order to insure adequate purification of the elements, the individual samples were recycled at least twice through the chemical procedures outlined here. Those cases in which the amounts of activity dealt with were notably low will be indicated.

Arsenic.—Precipitated (as As_2S_3) from 6*f* HCl and dissolved in NH_4OH solution; $GeCl_4$ removed by distillation from oxidizing medium; $AsCl_3$ subsequently distilled off under reducing conditions.

The 1.3-hour As^{78} as well as the 40-hour As^{77} were identified. By making two separations of the As fraction, the relative amounts of the As^{77} being formed from the 59-second and 12-hour isomers of Ge^{77}, respectively, could be determined. In two separations, small amounts of a 12-day activity were observed; however, it was not possible to characterize this isotope. Due to the small amounts of total activity present in many of the arsenic fractions separated (especially in the ones where low energy protons were used in the bombardments), statistical counting errors were as high as 50 percent.

TABLE II. Fission yield curve trough depths.

Proton energy (Mev)	Total yield of Cd^{115} / Yield of Sr^{89}
6.7	0.078±0.017
8.0	0.116±0.009
9.3	0.117±0.011
13.3	0.232±0.010
17.8	0.329±0.020
19.5	0.331±0.017
21.1	0.344±0.016

Bromine.—Oxidized to Br_2, Br_2 (and I_2) extracted into CCl_4; reduced with $NaHSO_3$, I^- oxidized to I_2 with $NaNO_2$, removed by CCl_4 extraction. Br^- subsequently oxidized to Br_2 and extracted into CCl_4, reduced with $NaHSO_3$ to I^- (aqueous solutions), precipitated as AgBr.

The 30-minute Br^{84} and 2.4-hour Br^{83} activities were detected in all bromine fractions; the 35-hour Br^{82} (shielded isotope) was identified in two samples where the activity of this isotope was sufficiently high to allow for its characterization.

Strontium.—Precipitated as $Sr(NO_3)_2$ with fuming

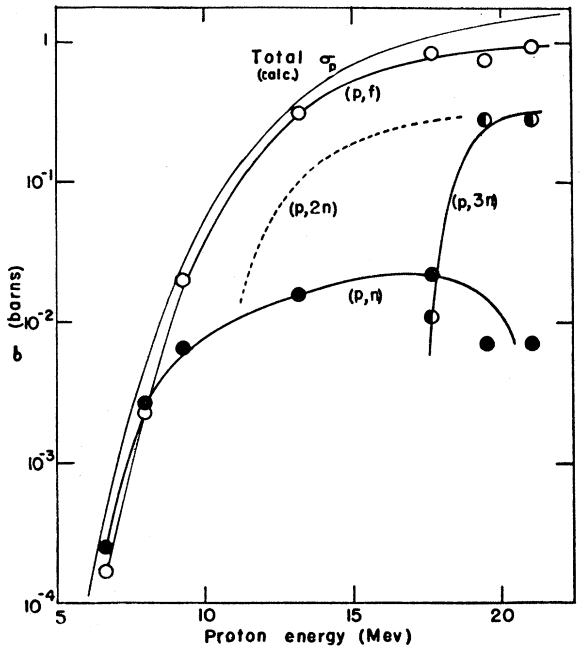

FIG. 9. Excitation functions for proton-induced reactions of Th^{232}.

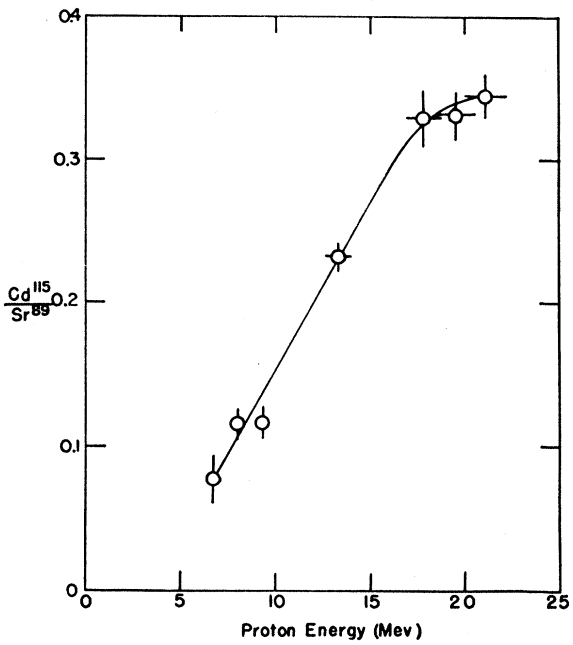

FIG. 10. Ratio of fission yield of Cd^{115} to that of Sr^{89} *vs* energy of incident protons.

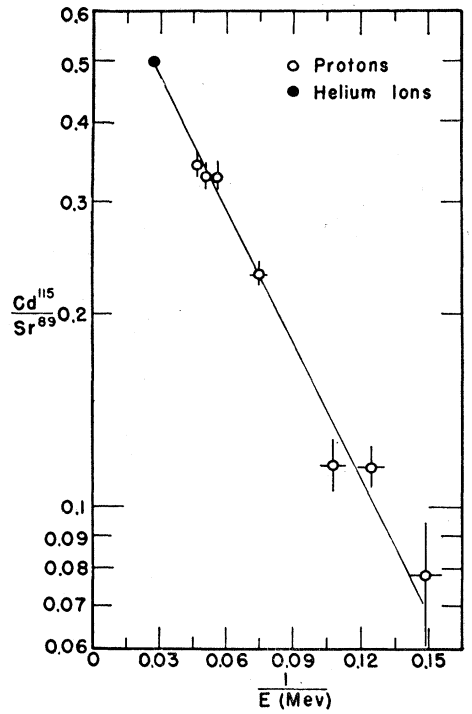

FIG. 11. Log of ratio of fission yields Cd^{115}/Sr^{89} *vs* reciprocal of incident proton energy.

HNO_3; redissolved and Ba removed by precipitating $BaCrO_4$. Scavenged with $Fe(OH)_3$, Sr finally brought down as SrC_2O_4.

The 9.7-hour Sr^{91} was identified in most samples. Also, a 50-day period was detected; this was assumed to be the isotope Sr^{89}, which has previously been reported to have a half-life of 53[13] or 55[14] days.

Zirconium.—Rare earth fraction removed as the fluorides, Ba added to bring down $BaZrF_6$. Precipitate redissolved using H_3BO_3, and concentrated acid; Zr finally precipitated as the cupferrate and ignited to ZrO_2.

Components of 17-hour, 1.3_2-day, 17.7-day, and 65-day periods were resolved after proton bombardments where energies of 18 Mev or higher were used. The 17-hour component was identified as Zr^{97} and the 65-day period assigned to Zr^{95}. These activities were present in all samples, regardless of the proton energies used. Likewise, the 1.3_2-day β^- activity, which proved to be Pa^{232}, was produced by protons of all energies. The 17.1-day period was identified as Pa^{230}; this isotope was produced only when protons of above 18-Mev energy were used. From the results of this work, it was concluded that protactinium was carried quantitatively by zirconium under the conditions used in making this separation. (See also section on Protactinium.)

Cadmium.—Precipitated as CdS from $0.2f$ HCl, redissolved, Fe, La, In scavengings made. CdS reprecipitated, redissolved, AgCl scavenging made. CdS again precipitated, redissolved, Pd and Sb separations run, CdS precipitated once more. Redissolved, final precipitation of $CdNH_4PO_4$.

The decay curves were separable into 2.19-day and 43-day activities, which were obviously identifiable with the two isomers of Cd^{115}. The 2.19-day half-life value was accurate to ~0.05 day, and differs slightly from that previously reported in the literature (2.33 days).[15]

Iodine.—Aliquot plus carrier oxidized with NaOCl to obtain all iodine in the same oxidation state. Reduced with NH_2OH, extracted into CCl_4. Reoxidized with $NaNO_2$, extracted with CCl_4. Reduced with $NaHSO_3$, AgI precipitated.

Both the 8.0-day I^{131} and 2.4-hour I^{132} (daughter of the 77-hour Te^{132}) were identified unambiguously.

Barium.—Precipitated as $Ba(NO_3)_2$ with fuming HNO_3. Redissolved, precipitated as $BaCrO_4$, dissolved in $6f$ HCl, precipitated as $BaCl_2$.

An 85-minute activity, identified as Ba^{139}, was found. The expected growth of the 40-hour La^{140} into secular equilibrium with the 12.8-day Ba^{140} was also observed.

Europium.—After removal of Th and Zr as the iodates, Ba and Sr hold-back carriers added, Ce and Eu precipitated with NH_4OH, Nb and Zr hold-back carriers added, CeF_3, EuF_3 precipitated. Redissolved in H_3BO_3—acid solution, Eu(III) reduced to Eu(II) in Jones reductor, and $Ce(OH)_3$ precipitated with NH_4OH. Eu finally obtained as $Eu_2(C_2O_4)_3$.

Decay curves with half-lives of 14.2 days were obtained; these were identified as resulting from the Eu^{156} activity present. This isotope has previously been reported as having a 15.4-day half-life.[16] Also, an unidentifiable ~57-day activity was noted in some samples. Due to the small amounts of total activity present in many of the europium fractions separated, statistical counting errors as great as 50 percent were encountered. (In some samples, especially those prepared from targets which had been bombarded with low energy protons, activities of less than 1 c/m above background were detected.)

Protactinium.—Zirconium carrier added, $16f$ HNO_3 added, solution taken to fumes. Diluted until $4f$ in

[13] Novey, Engelkemeier, Brady, and Glendenin, *Radiochemical Studies: The Fission Products* (McGraw-Hill Book Company, Inc., New York, 1951), Paper 76, National Nuclear Energy Series, Plutonium Project Record, Vol. 9, Div. IV.

[14] D. W. Stewart, Phys. Rev. **56**, 629 (1939).

[15] R. P. Metcalf, *Radiochemical Studies: The Fission Products* (McGraw-Hill Book Company, Inc., New York, 1951), Paper 127, National Nuclear Energy Series, Plutonium Project Record, Vol. 9, Div. IV.

[16] L. Winsberg, *Radiochemical Studies: The Fission Products* (McGraw-Hill Book Company, Inc., New York, 1951), Paper 198, National Nuclear Energy Series, Plutonium Project Record, Vol. 9, Div. IV.

HNO_3. Solution scavanged with I_2 in benzene, then Zr, Nb, and Pa extracted into benzene, 0.4f in TTA. Benzene phase ignited; resulting ZrO_2 solid mounted.

Same activities detected as in the zirconium fraction. As the ratios of the different activities detected were the same within experimental error as those found in the zirconium samples, it was concluded that protactinium was quantitatively carried in both procedures. The method of isolating Pa alone with Zr by two independent chemical procedures was adopted in order to determine the chemical yield without the necessity of adding Pa^{231} tracer.

PHYSICAL REVIEW VOLUME 88, NUMBER 4 NOVEMBER 15, 1952

Grain Boundary Barriers in Germanium*

W. E. TAYLOR,† N. H. ODELL,‡ AND H. Y. FAN
Purdue University, Lafayette, Indiana

(Received July 21, 1952)

High resistance at crystal grain boundaries in n-type germanium is investigated. The resistance is symmetrical with respect to the direct on of the current and resembles the characteristics of a rectifier in the blocking direction. Such barriers are also photosensitive. The barrier is eliminated when the material is converted to p-type by nucleon bombardment or heat treatment. A theory is developed assuming the existence of surface states at the boundary. The ability of the barriers to withstand high voltages, around 100 volts, is explained by showing that the surface charge increases with increasing voltage. The dc conductance of the barrier, measured at different temperatures, agrees with theory in the dependence on temperature as well as in the order of magnitude. At sufficiently low temperatures the barriers show a capacitance independent of the frequency, whereas at higher temperatures the barrier admittance is strongly frequency dependent. These results are in agreement with the theory, showing that at low temperatures the current across the boundary is mainly carried by electrons, the hole current becoming increasingly important as the temperature is raised. The height of the potential barrier above the Fermi level is determined and found to be independent of temperature. A small difference in the measured breakdown voltage for the two directions of current is attributed to a difference in impurity concentration on the two sides of the boundary, which is confirmed by the ac measurements. The number of electrons on the boundary states is found to be of the order 10^{12} cm^{-2} at the breakdown, which may be the saturation of the boundary states. However, the field at breakdown is only a few times lower than the critical value for the onset of the Zener current, and this mechanism cannot be definitely ruled out.

INTRODUCTION

GRAIN boundaries in n-type germanium are often found to present a high resistance to current flow in either direction.[1–4] Curve A, Fig. 1, shows the potential variation as measured by a whisker probe along a germanium sample with a grain boundary. The potential is seen to make an abrupt jump at the boundary, corresponding to 95 percent of the total potential difference applied to the sample. This high boundary resistance is not due to an insulating layer of foreign material. Microphotographs do not reveal any second phase at such boundaries. Furthermore, when a sample with a high resistance grain boundary is changed into p-type, either by nucleon irradiation[5] (curve B, Fig. 1) or by heating to high temperatures and subsequent quenching,[2] the boundary resistance vanishes. It reappears when the sample is changed back to n-type by annealing.

The resistance of the boundary is nonohmic, increasing with increasing voltage, and is approximately symmetrical regarding the direction of current. Figure 2 shows a set of typical current-voltage curves. The curve for both directions of current flow resembles the ordinary rectifier characteristic in the blocking direction. Furthermore, the grain boundary is also photosensitive; the photovoltage generated by a sharp pencil of light reverse its sign as the light crosses the boundary, and the signs are such as to agree with the picture of two potential barriers of a n-type semiconductor existing at the boundary back to back.[6] Merritt[7] and Benzer[8] have shown that two wedge-shaped pieces of uniform n-type germanium brought to a point contact give a current-voltage characteristic similar to the curve in Fig. 2. The nonohmic contact resistance was interpreted as due to potential barriers at free surfaces of n-type

* Work supported by a Signal Corps contract. The dc measurements are part of a thesis submitted by W. E. Taylor and the ac measurements are part of a thesis submitted by N. H. Odell to the faculty of Purdue University in partial fulfillment of the requirements for the Ph.D. degree.

† Now at Motorola Research Laboratory, Phoenix, Arizona.

‡ Now at Bell Telephone Laboratories, Allentown, Pennsylvania.

[1] K. Lark-Horovitz, NDRC Report 14–585 (1945) (unpublished).

[2] G. Pearson, Phys. Rev. **76**, 459 (1949).

[3] W. E. Taylor and H. Y. Fan, Phys. Rev. **78**, 335 (1950).

[4] N. H. Odell and H. Y. Fan, Phys. Rev. **78**, 334 (1950).

[5] W. Taylor and K. Lark-Horovitz, Purdue Semiconductor Research Progress Report (October, 1948) (unpublished); reference 3.

[6] M. Becker and H. Y. Fan, Purdue Semiconductor Research Progress Report (June, 1949); see also reference 2.

[7] E. Merritt, Proc. Natl. Acad. Sci. **11**, 743 (1925).

[8] S. Benzer, Phys.Rev. **71**, 141 (1947).